Mon. Not. R. Astron. Soc. **000**, 000–000 (0000) Printed 1 February 2008 (MN LATEX style file v1.4)

The discovery of very red counterparts to faint X-ray sources

A.M. Newsam,[1] I.M. McHardy,[1] L.R. Jones,[2,3] K.O. Mason[4]
[1] *Department of Physics and Astronomy, Southampton University, Southampton, SO17 1BJ.*
[2] *School of Physics and Space Research, University of Birmingham, Edgbaston, Birmingham B15 2TT.*
[3] *Code 660, NASA/GSFC, Greenbelt, MD 20771, USA.*
[4] *Mullard Space Science Laboratory, University College London, Holmbury St Mary, Dorking RH5 6NT.*

Submitted to MNRAS March 1997, Accepted August 1997

ABSTRACT

We present deep K-band imaging at the positions of four very faint X-ray sources found in the UK Rosat Deep Survey (McHardy *et al.* 1997) to have no optical counterpart brighter than R∼23. Likely identifications are found within the Rosat error circle in all four fields with R−K colours of between 3.2±0.4 and 6.4±0.6. From a consideration of the R−K colours and X-ray to optical luminosity ratios of the candidate identifications, we tentatively classify two of the X-ray sources as very distant ($z \sim 1$) clusters of galaxies, one as a narrow emission line galaxy and one as an obscured QSO.

Key words: cosmology:diffuse radiation – cosmology:observations – galaxies:active – galaxies:clusters.

1 INTRODUCTION

Optical identification of sources detected in deep X-ray images, particularly from the Rosat satellite, have, in recent years, proved a highly successful probe of the origins of the soft Cosmic X-ray background (XRB) (Shanks *et al.* 1991; Boyle *et al.* 1994; McHardy *et al.* 1997). In particular, it has been seen that at bright fluxes, the major class of contributors is QSOs. However, they are unlikely to contribute more than ∼50% of the X-ray background at 1keV (Boyle *et al.* 1994; Jones *et al.* 1996; McHardy *et al.* 1997) and, even were their contribution to increase greatly beyond the limits of current surveys, their characteristic X-ray spectrum is too soft to match the residual XRB (Romero-Colmenero *et al.* 1996). Deeper X-ray surveys, however, are showing that at fainter fluxes, there is a new class of galaxies with narrow optical emission lines (NELGs) which have suitably hard X-ray spectra (McHardy *et al.* 1995; Romero-Colmenero *et al.* 1996; Almaini *et al.* 1996).

The deepest X-ray survey yet optically identified is the UK Rosat Deep Survey. This reaches a depth of 2×10^{-15} erg cm^{-2} s^{-1} (0.5-2keV) and is described in detail in McHardy *et al.* (1997).

Within the "complete" sample area defined by McHardy *et al.* (1997), there are eleven unidentified sources (out of a total of 70 sources). Of the unidentified sources, most (7) remain unidentified because adequate optical spectra have not been obtained for all likely candidates. However, for four of the X-ray sources there are no optical candidates brighter than R ∼ 23. This is a puzzle since they are not primarily the faintest X-ray objects in the survey. One possibility is that the source of the X-rays are obscured AGN – long proposed as a contributor to the XRB (see for example Shanks *et al.* 1996). The discovery of such objects would have important implications for the origin of the hard X-ray background. The X-rays could also be coming from distant clusters of galaxies, which can have high X-ray to optical luminosity ratios (see, for example, Stocke *et al.* 1991). Other possibilities include further NELG objects or very high redshift QSOs, where the bright Lyα emission has been redshifted out of the R-band. All of these classes of objects, particularly the obscured AGN, will have red optical/infra-red colours, so in 1996 we performed deep K-band imaging at UKIRT of the four 'blank' Deep Survey fields to identify candidate objects and try to determine their nature. The results of this imaging are presented in this paper.

In section 2 we briefly describe the X-ray and optical data that make up the deep survey, in section 3 we present the K-band images and in 4, we consider possible scenarios. Finally in section 5 we discuss the possible significance of the results.

2 THE UK ROSAT DEEP SURVEY: OPTICAL IDENTIFICATIONS

The UK Rosat Deep Survey is a total of 115 ksec of Rosat position sensitive proportional counter (PSPC) observation

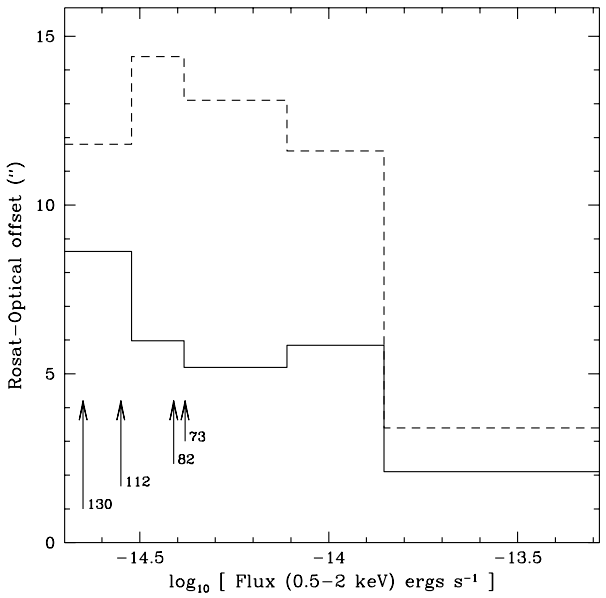

Figure 1. The offset between ROSAT positions and optical counterparts as a function of X-ray flux. The average offset in each flux bin is shown by the solid line, and the maximum offset by the dashed line. Only firm identifications are included, and galaxy clusters and groups are excluded because of the uncertainty that their extension introduces into the X-ray position. The flux bins are chosen to each contain a similar number of objects. The flux positions of the four blank field sources are shown.

of RA 13 34 37.0 Dec +37 54 44 (J2000) divided between two exposures — in June 1991 (Branduardi-Raymont *et al.* 1994) and June/July 1993. This region of sky was selected because of its extremely low obscuration — $N_H \sim 6.5 \times 10^{19}$cm^{-2}. Using these data, sources were identified at more than 3.5σ significance down to 1.6×10^{-15} erg cm^{-2} s^{-1}. Optical CCD images of the inner 15 arcmin radius of the ROSAT field taken at the University of Hawaii 88inch telescope were then used to find potential optical counterparts and subsequent spectroscopy has enabled identification of the sources in a statistically complete subsection making up about 80% of the 15 arcmin survey area down to 2×10^{-15} erg cm^{-2} s^{-1} (McHardy *et al.* 1997).

The majority of these sources are identified with QSOs, NELGs and galaxy clusters, and a small number with stars. However, of interest in this paper are four X-ray sources where the initial CCD imaging revealed no candidates within ~ 15 arcsec of the X-ray position brighter than R ~ 23. All four of these sources are towards the fainter flux end of this sample (ie $< 5 \times 10^{-15}$ erg cm^{-2} s^{-1}). However, even down at these faint limits, we have found from the offsets between the optical and X-ray positions of identified sources as shown in figure 1, that we would still expect the optical counterpart of the faintest of these sources to be within ~ 12 arcsec of the ROSAT position (90% confidence).

The source searching in the deep survey was based on the Cash statistic (Cash 1979) and is described in more detail in McHardy *et al.* (1997) and Branduardi-Raymont *et al.* (1994). Simulations showed that for sources detected at greater than 3.5σ significance, the survey is complete above a flux limit of 1.8×10^{-15} erg cm^{-2} s^{-1}. Therefore, even the faintest of the sources (r130 – see table 2) is detected at $> 3.5\sigma$.

Object Name	Total Exposure (secs)	Figure Number	Limiting K mag
r73	1620	3	∼20
r82	1620	4	∼20
r112	3240	5	∼20.5
r130	1320	6	∼20

Table 1. The details of the K-band images in figures 3 to 6. The limiting magnitudes refer to the central 140×140 pixel square region where all the images in the 9-position sampling pattern overlap.

In March 1995, the whole 15 arcmin radius ROSAT survey region was again imaged in the R band to a greater depth, using the University of Hawaii 8K×8K CCD array (Metzger, Luppino & Miyazaki 1995) on CFHT with a 1 hour exposure. This image revealed some possible optical candidates in two of the fields at R∼23, but nothing of note (ie R$\lesssim$24) in the other two (see the right hand panels of figures 3 to 6).

3 INFRA-RED IMAGING

The K-band images were obtained in one night in May 1996 at UKIRT using the IRCAM3 camera. The images in figures 3 through 6 were formed from multiple 9-point mosaics — hence the loss of quality towards the edges where fewer of the sub-images overlap. Total exposure times range from just over 20 mins to 1 hour (see table 1). Initial reduction was performed at the telescope using the IRCAM3_CLRED package, but the final images given here were re-reduced in IRAF using purpose-built codes. The seeing for the night was just greater than 1 arcsec and the pixels are 0.286 arcsec (the original K-band IRCAM3 images were 256×256 pixels, the mosaics created are 311×311 pixels).

The four K-band images are given in the left hand panels of figures 3 to 6, the right hand panels being the deepest available R-band images of the same areas for comparison. It should be noted that exposure times vary from image to image, and the grey-scale shading of each has been chosen individually for each image for clarity. Direct visual comparisons *between* the different K-band images should not, therefore, be made.

We will now look at the results for each of the fields individually. Table 2 gives the relevant X-ray and optical/IR details of the objects. The magnitudes given refer to the candidates discussed in the sections below.

3.1 Object r73

Object r73 is the X-ray brightest of the four sources (see table 2) and a very faint (R∼23) object can be seen close to the X-ray centroid in our deepest optical images (this can just be seen at the centre of the right hand frame of figure 3). The only other reasonable candidates are the pair of objects to the north (up) which are 20 and 21mag. However, these are both 20 arcsec from the X-ray centroid, which is far larger than the average positional offsets at this flux (cf figure 1).

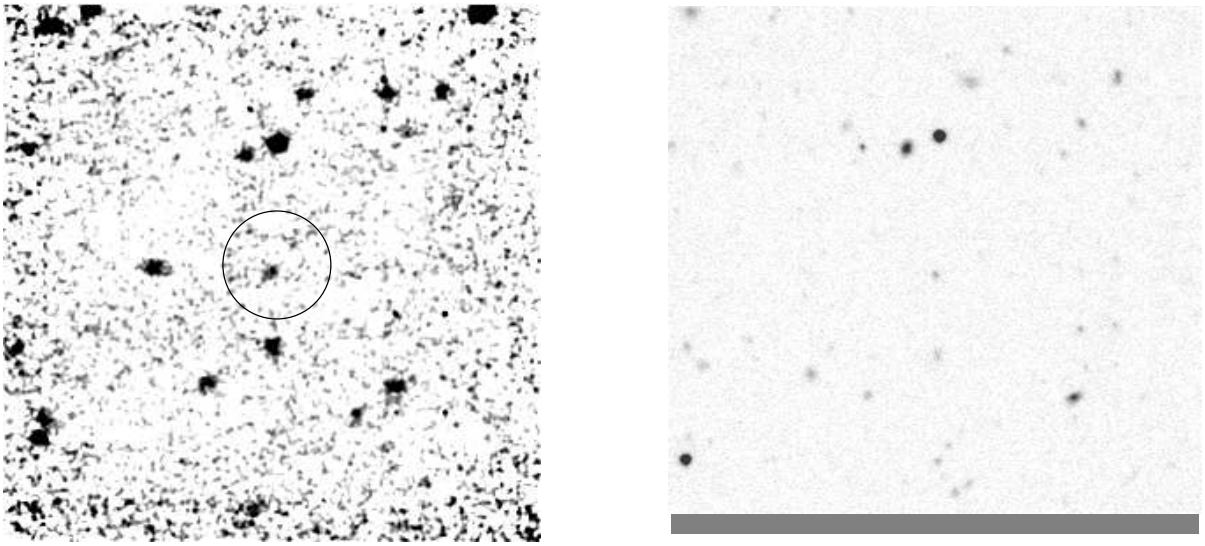

Figure 3. Object r73. In the left hand panel is shown the K-band image of object r73. The image has been smoothed slightly for clarity (with a gaussian with $1\sigma = 1$ pixel). A 10 arcsec radius error circle around the approximate ROSAT position is given and the object near the center is the one referred to in the text. The right hand panel has an R-band image for comparison. For both images, the north is to the top and east to the left. The K-band image has a limiting magnitude of K∼20 and the R-band image, R∼24.

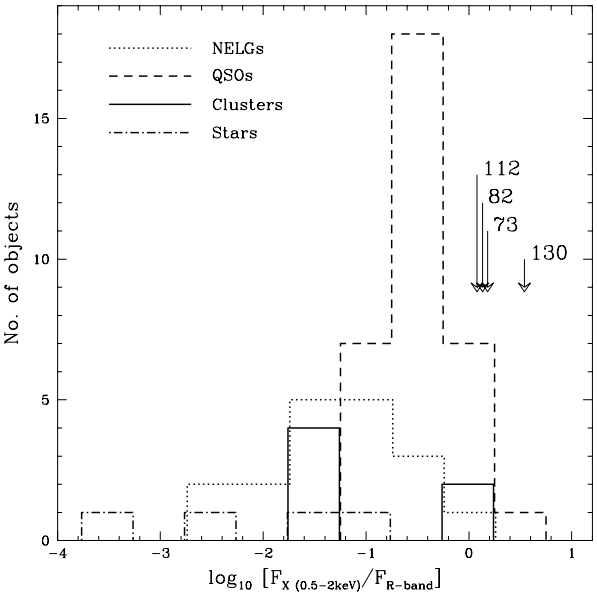

Figure 2. A comparison of the distribution of X-ray to optical flux ratios for the firmly identified QSOs, NELGs and stars in the Deep Survey and the ratios for the best candidates found in the blank fields. The histograms show the distributions of the three classes of known objects, with the positions of the four blank field candidates marked by arrows. The F_X is the integrated 0.5–2 keV ROSAT flux, and $F_{R\text{-band}}$ the optical R band flux.

The K-band image shows no additional candidates close to the X-ray centroid. A faint, red object (K∼18.6, R−K$\gtrsim$5) is visible to the east, but is again, nearly 20 arcsec from the centroid, so the central source is by far the most likely candidate. The relevant magnitudes for this central object are given in table 2.

3.2 Object r82

For object r82 there is a clear-cut candidate at the center of the X-ray error circle (marked in the left hand panel of figure 4) which is also just visible on the deep R-band image. The faintness of the candidate identifications in all of the K-band images prevents the reliable detection of extension, but the central object in the r82 image is certainly at least as compact as any other object in the image. The R−K colour of ∼4.2 is also redder than that of r73.

3.3 Object r112

Unlike the other sources, r112 has no single clear-cut candidate. Instead, several red objects, not visible in R, can be seen in the K-band image fairly close to the X-ray centroid (a 10 arcsec error circle around the centroid is shown in figure 5). The details in table 2 refer to the object just inside the bottom of the error circle, but the other nearby objects have similar colours (ie R−K∼ 4). The images are too faint to determine whether or not the candidates are significantly extended, but we are perhaps looking at a distant cluster (see sec. 4.3).

3.4 Object r130

The final optically blank X-ray source, r130, is the reddest object of all. There is very little to be found on the deep R-band image (figure 6), but a point-like object is seen on the edge of the 10 arcsec error circle in the K-band image (10 arcsec is quite a reasonable positional accuracy for an object this faint in X-rays — see figure 1). The object is

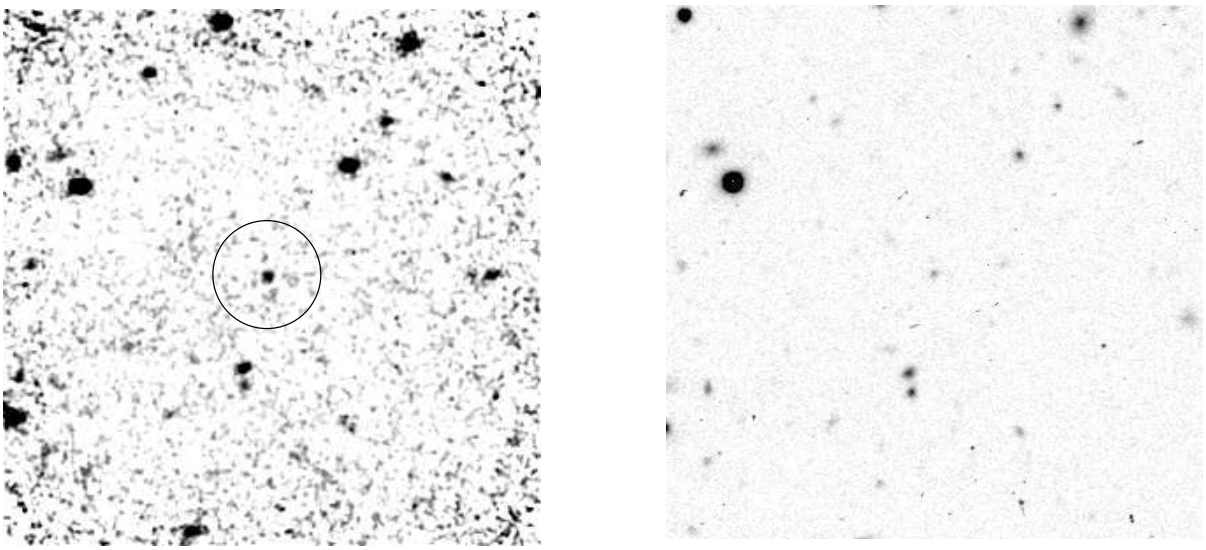

Figure 4. Object r82. As figure 3.

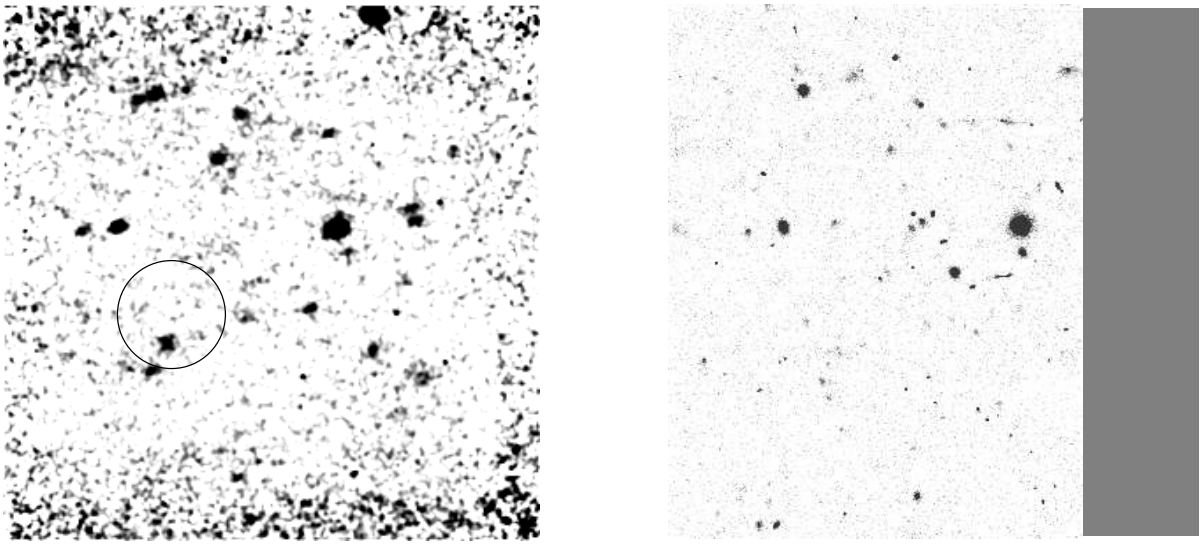

Figure 5. Object r112. As figure 3 but with slightly deeper K-band image (limiting K∼20.5).

extremely red — even though there is almost nothing to be seen in R, it is the brightest candidate object found in any of our fields at K. It also has an extremely high X-ray to optical flux ratio (see table 2 and figure 2).

4 POSSIBLE CLASSIFICATIONS

Although we cannot unambiguously classify the candidate objects with the current data, we can narrow down the range of possibilities considerably.

4.1 Stellar Sources

In figure 7 we compare the X-ray to optical luminosity ratios (L_X/L_{opt}) of the four candidates described above with the ratios found for various classes of X-ray sources in the Einstein Medium Sensitivity Survey (EMSS) by Stocke *et al.* (1991). It is clear from this figure that a stellar origin for the X-rays in any of the four blank fields can almost certainly be ruled out. Although not shown in Stockes figure, it is perhaps possible that we are looking at very faint cataclysmic variable (CV) systems, with the K-band emission dominated by a faint M-dwarf companion. Such systems can give very high L_X/L_{opt} values.

Although we do not have sufficient data to separate the contribution to the measured brightness of the accretion disk and M-dwarf components, Sproats, Howell & Mason (1996) give a distance estimation technique for CVs which we can use to get lower limits on the distances for the four candidates. To do this we will assume that the M-dwarfs all have

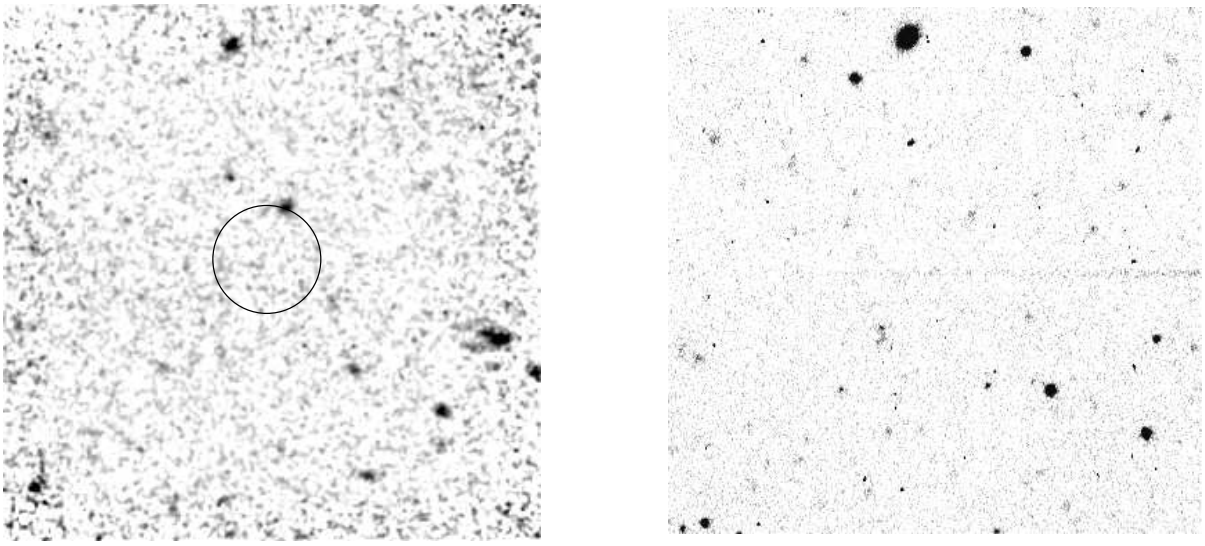

Figure 6. Object r130. As figure 3.

Object Name	ROSAT flux (0.5 – 2 keV) (erg cm^{-2} s^{-1})	ROSAT position (J2000) RA	Dec	K mag.	Optical position (J2000) RA	Dec	R−K	log[F_X/F_{opt}] (R band)
r73	4.13×10^{-15}	13 35 16.99	37 54 18.9	19.7 ± 0.25	13 35 17.2	37 54 16	3.2 ± 0.4	0.18
r82	3.85×10^{-15}	13 35 15.83	37 52 41.1	18.7 ± 0.25	13 35 15.9	37 52 41.1	4.2 ± 0.4	0.13
r112	2.81×10^{-15}	13 34 27.64	37 54 22.7	18.9 ± 0.25	13 34 27.5	37 54 14	4.2 ± 0.4	0.08
r130	2.25×10^{-15}	13 33 43.40	37 50 32.1	18.4 ± 0.25	13 33 43.1	37 50 42.0	6.1 ± 0.6	0.54

Table 2. X-ray, optical and IR data for the candidate objects for each 'blank' field as identified in sections 3.1 to 3.4.

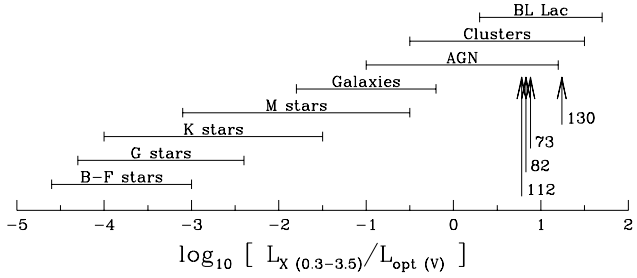

Figure 7. The horizontal bars show the ranges of log[L_X/L_{opt}] found by Stocke *et al.* (1991) in the EMSS. For comparison, the log[L_X/L_{opt}] of the blank fields are given. The optical flux for clusters is derived from the brightest cluster galaxy. The L_X/L_{opt} values for the blank fields have been converted from 0.5–2.0 keV to the 0.3–3.5 keV band used by Stocke assuming a spectral slope of 1.0 and converted from R to the V-band used by Stocke assuming a V−R of 1.

radii greater than 0.1 solar radii (see Caillault & Patterson 1990) and that the maximum V−R colour for the objects is 4 (Ramseyer 1994). Under these assumptions we find that r130 is $\gtrsim$ 200 pc away, r82 and r112 both $\gtrsim$ 350 pc and r73 $\gtrsim$ 700 pc. The Deep Survey pointing is almost directly out of the galactic plane and Van Paradijs, Augusteijn & Stehle (1996) find an exponential scale height for CVs of $\sim$ 200pc. Therefore r130, r112 and r82 could all be within a reasonable distance of the plane. Nevertheless, the rarity of comparable known objects (eg Kolb 1993) means that this must be considered an intriguing but largely unsupported possibility.

4.2 Galaxies and NELGs

In none of the K-band images are the likely candidate objects significantly extended, however this is mainly due to the faintness of the sources and the large IR background which makes modelling of the profile difficult. Therefore, we cannot use apparent extension as a means of identifying galaxies. The range of L_X/L_{opt} values for "Normal Galaxies" taken from by Stocke *et al.* (1991) in figure 7 is well away from the ratios found for the blank fields, but this classification does not include the NELGs found in the Deep Survey. As can be seen in figure 2, these have X-ray to optical ratios that are similar to those of AGN and are, therefore, much closer to the values for the blank field candidates than normal galaxies. It is also important to remember that these fields have, in essence, been *selected* because of their high L_X/L_{opt} and it is not unreasonable to suppose that they will fall towards the higher end of the distribution of L_X/L_{opt} for their particular object type.

In addition, the R−K colour of object r73 of 3.2 is consistent with the NELGs and, indeed, with most galaxies with $z \ll 1$ (Steidel & Dickinson 1995). We have K magnitudes for a handful of confirmed NELGs, and all have R−K between 3 and 3.5. However, the R−K of 4.2 for objects r82 and r112 is less reasonable and R−K of $\sim$ 6 for r130 is too extreme.

Object Name	R-band mag.	Redshift z (estimate)	log[L_X] (0.5-2 keV) erg sec^{-1}
r73	22.9	0.8	43.0
r82	22.9	0.8	43.1
r112	23.1	0.9	42.9
r130	24.5	1.1	43.1

Table 3. Estimated redshifts and X-ray luminosities of the four X-ray sources under the assumption that the candidate objects are the brightest members of a galaxy cluster. Distance estimate calibration and K-corrections are taken from Schneider, Gunn & Hoessel (1983) with the K-corrections linearly extrapolated slightly above $z = 1$.

4.3 Clusters of Galaxies

The L_X/L_{opt} values for the blank field objects fall comfortably into the range found for clusters of galaxies, but is the same true for the R-K colours? If the X-ray emission from the objects is associated with a cluster, then the candidate identifications will probably be the brightest cluster galaxies (BCG). Under this assumption, we can use the apparent magnitude of the object to estimate the redshift of the cluster and therefore check that the R-K colours and absolute X-ray luminosity are reasonable.

Using the BCG calibration and K-corrections from Schneider, Gunn & Hoessel (1983) we obtain the estimated redshifts and X-ray luminosities found in table 3. Estimated redshifts for the four objects are between 0.8 and 1.1, with L_X values all around 10^{43} erg sec^{-1}. Other clusters and galaxy groups in the survey have log[L_X] between 42 and 43.5 erg sec^{-1} so all the candidates in the blank fields are compatible with these. In addition, from Steidel & Dickinson (1995) we find that model galaxy spectra of elliptical galaxies give R-K colours of $\sim$5 at $z = 0.8$ up to $\sim$6 at $z = 1.1$ which, given the scatter that is seen around the model value, is again consistent with the R-K values found for all the candidates (refer to table 2).

Therefore, a $z \sim 1$ galaxy cluster origin cannot be ruled out for any of the blank fields.

4.4 AGN

Typically, AGN have fairly blue R−K colours of ~ 2, rarely going above 3 (see, for example, Dunlop *et al.* 1986 figure 2). Therefore, the very red colours of the candidate objects found, particularly of r82, r112 and r130, would seem to exclude AGN as the source of the X-rays. However, such colours might be seen in AGN under some circumstances.

For example, it is possible that this colour is a result of a very high redshift. At $z > 5$, Ly$_\alpha$ passes out of the R band, giving a very red colour. This would make all four of the sources by far the most X-ray luminous in the Deep Survey. While this is not impossible, it is unlikely to be the case for all four sources and so, perhaps more realistically, we should consider the possibility of intrinsic reddening. It has frequently been suggested that obscured AGN could contribute a significant part of the XRB at a large range of energies, not just the soft X-ray band (eg Madau *et al.* 1994; Comastri *et al.* 1995). The recent discovery by Shanks *et al.* (1996; see also Almaini *et al.* 1995) of an X-ray source with narrow optical emission lines, but a broad IR H$_\alpha$ has provided a probable member of this class of object. The object (Rosat object RXJ13434+0001 is also reddened with R−K$\sim$ 4.5 and an F_X/F_{opt} of ~ 0.45 in the same units as table 2). This is similar to object r82 and r130 could be an even more highly obscured AGN.

The amount of reddening required to give the observed colour will depend to some extent upon redshift. For example, to produce an observed R−K colour of 6 for an object with an intrinsic colour of 2 requires an N_H column of $\sim 10^{21.8}$cm^{-2} at a redshift of $z = 1$. (For this and subsequent calculations we assume a dust to gas ratio of 5.8×10^{21} cm^{-2} mag^{-1} taken from Bohlin, Savage & Drake 1978). This would take the intrinsic log[L_X/L_{opt}] of r130 down to ~ -3 — far too low for an extra-galactic object. On the other hand, the same observed colour for an object at $z = 2$ would need $N_H \sim 10^{21.5}$cm^{-2} which gives an intrinsic log[L_X/L_{opt}] for r130 of only -1, which although low is certainly acceptable for an AGN (see figure 7).

For objects r82 and r112 a lower column is required to produce the observed R−K colours. A distance of $1 \lesssim z \lesssim 3$ would be reasonable to produce an intrinsic L_X/L_{opt} suitable for an AGN with an N_H of between $\sim 10^{21}$ and $10^{21.5}$ cm^{-2}.

Alternatively, we could be looking at BL Lacs. These have redder colours than other AGN, typically in the range $2 \lesssim$ R−K $\lesssim 4.5$ (eg Cruz-Gonzalez & Huchra 1983) and high L_X/L_{opt} values (see figure 7). Therefore, only the R−K of 6.1 for r130 is too red. However, BL Lacs should be detectable in the radio, but deep 20cm and 6cm radio observations of the Deep Survey region at the Very Large Array (VLA) show no signs of radio sources down to the detection limit (~ 0.3 mJy) for any of the four blank fields.

5 CONCLUSIONS

We have used deep K-band imaging to attempt to identify the optical candidates of four faint X-ray sources with 'blank' optical fields (ie nothing within $\sim$ 15 arcsec of the X-ray centroid with R$\lesssim$23). Of the four fields, firm candidates have been found in three. The remaining field (object r112; figure 5) shows a collection of similar, red objects in the vicinity of the X-ray centroid. No firm conclusions about the nature of the candidates can be achieved with just the current photometric data but we have, nevertheless, been able to draw tentative conclusions.

Of the four X-ray sources, r73 has the least red candidate. In fact, both its R−K colour (3.2) and X-ray to optical luminosity ratio are entirely consistent with the Narrow Emission Line Galaxies (NELGs) found in significant quantities at the fainter end of the UK Rosat Deep Survey (M^{c}Hardy *et al.* 1997).

On the other hand, both r112 and r130 have candidates that are redder than in r73 (r112 has an R−K of 4.2, r130 has R−K of 6.1). These objects are probably better described by high redshift ($z \sim 1$) galaxy clusters, the candidates having absolute magnitudes, R−K colours and L_X/L_{opt} ratios consistent with typical $z \sim 1$ brightest cluster galaxys (BCGs). The collection of red objects in r112 also supports this conclusion.

The candidate object for source r82 also is also consistent with being a distant brightest cluster galaxy. However,

in this case both the deep R and K-band images show an apparently point-like object. It may therefore also be explained as a distant ($z \sim 2$) intrinsically reddened AGN. If this is the case, with this deep ROSAT observation, and others like it, we are just starting to see the tip of the iceberg which has been proposed as a significant contributor to the cosmic X-ray background, not just in the soft band, but over a wide range of energies (eg Madau *et al.* 1994).

Future observations will be required to confirm these tentative identifications. In particular, infra-red spectroscopy over a range of wavelengths would enable one to search for broad, redshifted emission lines characteristic of QSOs (a QSO with a redshift of $z \sim 2$ would have Hα redshifted into the H or K band). Further IR photometry in other bands to give IR colours may also prove a useful diagnostic and deeper imaging with good seeing would allow spatial extension to be seen if any of the objects are NELGs or moderate redshift clusters (ie $z \ll 1$).

Deep IR imaging, therefore, has shown itself to be a powerful tool in the study of the faintest X-ray sources. In all four of the optically blank fields containing X-ray sources which we have observed in the K-band, firm candidates have been found. In addition, consideration of the photometric and X-ray properties of the candidates has enabled us to make preliminary identifications of the types of objects producing the X-ray emission, and possibly identified an obscured QSO — a much hypothesised but little observed contributor to the cosmic X-ray background.

ACKNOWLEDGMENTS

Thanks to Tom Marsh for discussions about possible galactic identifications and to the referee for his encouraging comments.

The United Kingdom Infrared Telescope (UKIRT) is operated by the Joint Astronomy Centre on behalf of the U.K. Particle Physics and Astronomy Research Council.

IRAF is distributed by the National Optical Astronomy Observatories, which are operated by the Association of Universities for Research in Astronomy, Inc., under cooperative agreement with the National Science Foundation.

REFERENCES

Almaini, O., Boyle, B.J., Griffiths, R.E., Shanks, T., Stewart, G.C., Georgantopoulos, I., 1995, MNRAS, 277, L31.

Almaini, O., Shanks, T., Boyle, B. J., Griffiths, R. E., Roche, N.; Stewart, G. C., Georgantopoulos, I., 1996, MNRAS, 282, 295.

Bessell, M.S., 1991, Astron. J., 101, 662.

Bohlin, R.C., Savage, B.D., Drake, J.F., 1978, ApJ, 224, 132.

Boyle, B.J., Shanks, T., Georgantopoulos, I., Stewart, G.C., Griffiths, R.E., 1994, MNRAS, 271, 639.

Boyle, B.J, M^{c}Mahon, R.G., Wilkes, B.J., Elvis, M., 1995, MNRAS, 276, 315.

Branduardi-Raymont, G., et al., 1994, MNRAS, 270, 947.

Caillault, J-P., Patterson, J., 1990, Astron. J., 100, 825.

Cash, W., 1979, ApJ, 228, 939.

Comastri, A., Setti, G., Zamorani, G., Hasinger, G., 1995, A&A, 296, 1.

Cruz-Gonzalez, I., Huchra, J.P., 1983, ApJ, 89, 441.

Dunlop, J.S., Downes, A.J.B., Peacock, J.A., Savage, A., Lilly, S.J., Watson, F.G., Longair, M.S., 1986, Nature, 319, 564.

Jones, L.R. *et al.* 1995. Proc 35th Herstmonceux Conf., ed Mattox, S.

Jones, L.R., M^{c}Hardy, I.M., Merrifield, M.R., Mason, K.O., Smith, P.J., Branduardi-Raymont, G., Newsam, A.M., Dalton, G., Rowan-Robinson, M., Luppino, G., 1996, MNRAS (in press).

Kolb, U., 1993, A&A, 271, 149.

Madau, P., Ghisellini, G., Fabian, A.C., 1994, MNRAS, 270, L17

M^{c}Hardy, I.M. *et al.*, 1995, MPE Report 263, Proceedings of 'Röntgenstrahlung from the Universe', p331.

M^{c}Hardy, I.M. *et al.*, 1997, MNRAS (submitted).

Metzger, M.R., Luppino, G.A., Miyazaki, S., 1995, BAAS, 187, 73.

Van Paradijs, J., Augusteijn, T., Stehle, R., 1996, A&A, 312, 93.

Ramseyer, T.F., 1994, ApJ, 425, 243.

Romero-Colmenero, E., Branduardi-Raymont, G., Carrera, F.J., Jones, J.R., Mason, K.O., M^{c}Hardy, I.M., Mittaz, J.P.D., 1996, MNRAS, 282, 94.

Schneider, D.P., Gunn, J.E., Hoessel, J.G., 1983, ApJ, 264, 337.

Shanks, T., Georgantopoulos, I., Stewart, G.C., Pounds, K.A., Boyle, B.J., Griffiths, R.E., 1991, Nature, 353, 315.

Shanks, T., Almaini, O., Boyle, B.J., Della-Ceca, R., Done, C., Georgantopoulos, I., Griffiths, R.E., Rawlings, S.J., Roche, N., Stewart, G.C., MPE Report 263, Proceedings of 'Röntgenstrahlung from the Universe', p341.

Sproats, L.N., Howell, S.B., Mason, K.O., 1996, MNRAS, 282, 1211.

Steidel, C.C., Dickinson, M., in 'Wide Field Spectroscopy and the Distant Universe', 1995, p349.

Stocke, J.T., Morris, S.L., Gioia, I.M., Maccacaro, T., Schild, R., Wolter, A., Fleming, T.A., Henry, J.P., 1991, ApJS, 76, 813.